Influence of creep on dynamic behavior of concrete filled steel tube arch bridges

Yishuo Ma [1,2a], Yuanfeng Wang [*1], Li Su [1b] and Shengqi Mei [1c]

[1] *School of Civil Engineering, Beijing Jiaotong University,*
No. 3 Shangyuancun Road, Haidian District, Beijing, 100044, P.R. China
[2] *Center of Science and Technology of Construction, Ministry of Housing and Urban-Rural*
Development (MOHURD), No. 9 Sanlihe Road, Haidian District, Beijing, 100835, P.R. China

Abstract. Concrete creep, while significantly changing the static behaviors of concrete filled steel tube (CFST) structures, do alter the structures' dynamic behaviors as well, which is studied quite limitedly. The attempt to investigate the influence of concrete creep on the dynamic property and response of CFST arch bridges was made in this paper. The mechanism through which creep exerts its influence was analyzed first; then a predicative formula was proposed for the concrete elastic modulus after creep based on available test data; finally a numerical analysis for the effect of creep on the dynamic behaviors of a long-span half-through CFST arch bridge was conducted. It is demonstrated that the presence of concrete creep increases the elastic modulus of concrete, and further magnifies the seismic responses of the displacement and internal force in some sections of the bridge. This influence is related closely to the excitation and the structure, and should be analyzed case-by-case.

Keywords: creep; seismic analysis; time-dependent analysis; concrete; steel; arch bridges

1. Introduction

Concrete filled steel tube (CFST) as a competitive composite material has been widely used in various types of structures such as subway stations and ultra-high-rise buildings. Especially, its use in arch bridges has gained a rapid development in China (Wang *et al.* 2008). Nowadays, interest in the issue of bridge ageing has been greatly aroused (O'Byrne *et al.* 2013, Huang *et al.* 2010, Graf *et al.* 2010). In particular, the construction and operation of more than 300 CFST arch bridges in the last 20 years have necessitated the investigation into the creep effects on CFST arch bridges (Wang *et al.* 2008, Shao *et al.* 2010, Ma and Wang 2013, Ma 2013, Wang *et al.* 2013).

In terms of the influence of concrete creep on CFST arch bridges, most investigations have been conducted in static field. General consensus has been achieved that creep could cause a continuous change in the deformation and distribution of internal forces between the steel tube and the concrete core in CFST arch bridges, with the result that those long-term effects could even

∗Corresponding author, Professor, E-mail: cyfwang@bjtu.edu.cn
[a] Ph.D., E-mail: maysh@126.com
[b] Ph.D. Student, E-mail: su_bjtu@163.com
[c] Ph.D. Student, E-mail: woshimeishengqi@163.com

reach 50% of the instantaneous elastic responses produced upon stress application (Wang *et al.* 2008, Shao *et al.* 2010, Wang *et al.* 2013), bringing about a negative influence on both serviceability and safety of CFST arch bridges (Ma and Wang 2013, Ma 2013).

As for the influence of concrete creep that might be caused on the dynamic behavior of CFST arch bridges, there are only very few studies (Ma 2013, Ma *et al.* 2011), owing to that the conventional understanding on creep simply regards structural creep effects as a static problem while fails to relate it to dynamic field. Actually, static and dynamic performances, being two aspects of a structure, are not in isolation.

Dynamic time-history analysis involving geometric and material nonlinearities of structures under non-uniform excitations has become the mainstream in the research of seismic response of CFST arch bridges at present (Ghodrati Amiri *et al.* 2012, Aldemir *et al.* 2012, Qin and Faber 2012, Wu *et al.* 2006). It is to be noted, however, that for reinforced concrete or concrete-containing composite structures, either nonlinear or linear seismic behavior takes place actually on the basis of creep behavior due to the sustained loading effect anterior to an earthquake action. Being a typical aging viscoelastic material (Alizadeh *et al.* 2010), concrete exhibits obvious time-dependent properties that would inevitably exert a continuous influence on reinforced concrete and composite structures. Performing a seismic response analysis without taking the concrete creep effects into account, not only would make it difficult to reflect the actual condition of a bridge but also would reduce the significance of the use of the precise time-integration method.

The emphasis of this paper is laid on the influence of concrete creep on the dynamic behavior of CFST arch bridges. However, although the study deals mainly with the relation between creep and structural performance of the bridges, it should be mentioned that primarily there is a close relationship between creep and the material properties of the concrete, which is specifically taken to mean the material mechanical properties of the concrete after creep. Of particular attention in this respect is the concrete elastic modulus after creep in this study, which obviously plays an important part in structural dynamic analysis after creep.

The previous studies (Ma *et al.* 2011, Sapountzakis and Katsikadelis 2003) on the creep influence on dynamic behavior of structures considered a long-term effective modulus of concrete to be the material parameter for structural dynamic analysis. This paper makes a discussion on this point in detail and presents available experimental studies towards the end of rationally determining the elastic modulus of concrete after a period of creep. In general, the relationship between creep and material mechanical properties of concrete as well as structural deformation and internal forces is investigated first in this paper, and then followed by a structural seismic analysis on that basis.

2. Mechanism of the influence of creep on dynamic behavior of structures

From a more essential viewpoint, the creep influence on structural dynamic behavior, which is of particular interest in this paper, is the influence of a sustained loading on structural dynamic behavior in nature. Sustained loading and instantaneous loading may be said to be two totally different actions for concrete, having effects of a large difference. Objectively speaking, the knowledge of the influence of a sustained loading on concrete material and concrete structures is still inadequate at present, which is normally restricted to the development of deformation and internal forces, viz. the so-called creep effects. However, it should be added that a sustained loading would further exert an effect on the material mechanical properties of concrete, i.e., the

concrete would have a change in elastic modulus, strength and constitutive relationship after a period of sustained loading (Wang and Zhang 2009, Zhang *et al.* 2010), which is called as after-effect of creep in this paper.

Interpretation of the above statement reveals that the general influence of creep, or rather sustained loading, on concrete structures is twofold: that on deformation and internal forces of structures, and that on basic material mechanical properties. And these two aspects are the starting point from where this paper conducts the analysis on the dynamic performance of structures after a period of creep behavior.

It is important to clarify that the elastic modulus used for a structural dynamic analysis ought to be the tangent modulus of concrete which is obtained under an instantaneous load. For concrete subjected to a sustained load, some structural creep analysis methods have proposed various forms of effective modulus of concrete taking advantage of the concept of elastic modulus, such as the age-adjusted effective modulus defined in Trost-Bažant method (Bažant 1972, 1988). Such an effective modulus, being far different from the instantaneous elastic modulus of concrete, is relevant to a long-term deformation history of the concrete under a sustained load and applies to estimate structural creep effects such as time-dependent deflection and internal forces. Therefore the concrete elastic modulus involving the influence of sustained loading to be investigated experimentally and used in the dynamic analysis after creep in this study is not any form of effective modulus of concrete; instead, it should be an instantaneous elastic modulus measured by the standard test method after a long-term sustained loading.

3. Formulation of the elastic modulus of concrete after creep

To determine the influence of creep, the elastic modulus of the concrete having been loaded for 30 days, 60 days, 180 days and 360 days was tested by the authors' group (Ma 2013). Besides, the creep effect on the elastic modulus of concrete was also reported by researchers Davis and Davis (1931), Washa and Fluck (1950) and Cook and Chindaprasirt (1980). All these four groups of tests provide a consistent evidence for the effect of sustained loading on increasing the elastic modulus of concrete. In essence, a certain level of damage occurs in concrete inevitably during a sustained loading. On the other hand, a sustained loading also produces a time-dependent redistribution of stress concentrations in the cement paste and a consolidation process in the gel structure, leading to an acceleration of the solidification of concrete, i.e., a sustained loading has an intensifying effect involving both physical and chemical processes on concrete. On condition that the sustained load maintains within a certain level and the damage effect caused by the sustained loading is weaker than its intensifying effect, concrete would gain in mechanical properties.

Based on the four groups of tests mentioned above, a regressive formula describing the effect of sustained loading on concrete elastic modulus can be given as

$$\beta_{c,sus}(t,t_0) = 0.147 f_{cm}^{-0.03} \ln(3051.042 + t - t_0) \tag{1}$$

where $\beta_{c,sus}(t, t_0)$ is the ratio between the elastic modulus of a concrete after a period of sustained loading and that of an identical concrete not previously loaded; f_{cm} is the 28-day cylindrical compressive strength of concrete (MPa); $t - t_0$ is the loading duration (d); t_0 is the age at loading (d). The comparison between the regression and the test data is shown in Table 1.

From Table 1 it can be seen that the increasing rule of the elastic modulus is not very clear,

Table 1 Comparison between regression and test data of creep effect on elastic modulus

Data source	$t - t_0$ (d)	f_{cm} (MPa)	$\beta_{c,sus}$		Error (%)
			Test data	Regression	
Cook and Chindaprasirt (1980)	30	45.9	1.05	1.0528	0.03
	30	45.0	1.13	1.0534	7.01
	30	36.0	1.05	1.0605	0.59
	30	28.9	1.08	1.0675	1.23
Test by the authors' group	30	44.5	1.04	1.0537	1.37
	60	44.5	1.05	1.0550	0.43
	180	44.5	1.05	1.0600	1.32
	360	44.5	1.04	1.0671	2.94
Davis and Davis (1931) [*]	120	41.5*	1.03	1.0598	2.89
	330	39.9*	1.06	1.0695	0.89
Washa and Fluck (1950)	3860	27.5	1.13	1.1766	4.15
	3860	15.7	1.16	1.1965	2.73
	3860	10.6	1.20	1.2109	0.87

*Davis and Davis (1931) did not give the 28-day compressive strength of concrete. The values in the table are the compressive strength of the companion load-free specimens which had the same age and curing condition as the creep specimens

since there exist differences in concrete composition, vibrating method, specimen size, and temperature and humidity condition of the tests by different researchers. The ratio $\beta_{c,sus}(t,t_0)$ is obviously not a function with a single parameter of the sustained loading duration t-t_0. In view of the comparison between the regression and the test data, the formula based on the two parameters of sustained loading duration and concrete compressive strength fits well, with the maximum error of 7.01% and the average error of 2.03%.

According to CEB-FIP Model Code 2010 (FIB 2010), the development of concrete elastic modulus due to aging can be estimated by

$$E_c(t) = \beta_E(t)E_{c,28} \tag{2}$$

where $E_c(t)$ is the elastic modulus of a load-free concrete at an age t; $E_{c,228}$ is the 28-day elastic modulus of concrete; $\beta_E(t)$ is a coefficient which depends on the age of concrete. The concrete elastic modulus reckoning in sustained loading $E_{c,sus}(t, t_0)$ can thus be evaluated as

$$E_{c,sus}(t,t_0) = \beta_{c,sus}(t,t_0)\beta_E(t)E_{c,28} \tag{3}$$

4. Computational of the creep of CFST arch bridges

4.1 Description of the time-dependent strain of concrete

Model B3 for concrete creep (Bažant and Baweja 2000) is adopted in this paper, which is based

on the solidification theory (Bažant and Prasannan 1989a, b) and takes into account various parameters such as the cement content, water/cement ratio, aggregate/cement ratio and compressive strength of the concrete. Model B3 distinguishes creep into basic and drying ones as

$$J(t,t_0) = q_1 + C_0(t,t_0) + C_d(t,t_0,t') \tag{4}$$

where $J(t, t_0)$ is the compliance function, which is taken as elastic plus creep strain caused by a unit uniaxial constant stress (10^{-6}/MPa); q_1 is the instantaneous strain due to a unit stress; $C_0 (t, t_0)$ is the compliance function for basic creep (10^{-6}/MPa); $C_d (t, t_0, t')$ is the additional compliance function due to simultaneous drying (10^{-6}/MPa); t is the target time (d); t_0 is the age at loading (d); t' is the age when drying begins (d).

Seeing that the sealing action provided by the steel tube protects the concrete from the migration and loss of moisture, and considerably reduces shrinkage and drying creep of the concrete, we lay emphasis simply on basic creep in this paper (Shao *et al.* 2010, Terrey *et al.* 1994, Naguib and Mirmiran 2003), which is characterized in Model B3 by

$$C_0(t,t_0) = q_2 Q(t,t_0) + q_3 \ln[1 + (t-t_0)^n] + q_4 \ln(\frac{t}{t_0}) \tag{5}$$

where q_2, q_3, and q_4 = aging viscoelastic compliance, non-aging viscoelastic compliance, and flow compliance concerning the composition and strength of concrete respectively, as deduced from the solidification theory; $Q(t, t_0)$ = a function concerning the age at loading; n = empirical parameter.

The creep coefficient of concrete $\varphi(t, t_0)$ needed in the following analysis, defined as the ratio of net creep strain to initial elastic strain, can then be evaluated in terms of elastic modulus at initial time $E(t_0)$ and creep compliance function $J(t, t_0)$ as

$$\varphi(t,t_0) = J(t,t_0)E(t_0) - 1 \tag{6}$$

4.2 Finite element model of structural creep

As a consequence of creep, the internal forces and stresses of the concrete core and steel tube in a CFST arch bridge vary with time even under a constant load. The total strain $\varepsilon(t)$ of concrete caused by a sustained variable stress (initial value $\sigma(t_0)$) can be calculated based on the principle of superposition, which is usually assumed to apply to concrete within the linear creep range, i.e., for the applied stress less than about 0.4 times of the concrete strength (Bažant 1988), as

$$\varepsilon(t) = \frac{\sigma(t_0)}{E(t_0)}[1 + \varphi(t,t_0)] + \int_{t_0}^{t} \frac{1}{E(\tau)} \frac{d\sigma(\tau)}{d\tau}[1 + \varphi(t,\tau)]d\tau \tag{7}$$

Assuming that the strain history of concrete varies in proportion to creep coefficient $\varphi(t, t_0)$, the above creep stress-strain relationship can be transformed to the following incremental form based on the age-adjusted effective modulus method (Bažant 1972) as

$$\Delta\varepsilon(t) = \frac{\Delta\sigma(t)}{E_\varphi(t,t_0)} + \frac{\sigma(t_0)}{E(t_0)}\varphi(t,t_0) \tag{8}$$

$$E_\varphi(t,t_0) = \frac{E(t_0)}{1 + \chi(t,t_0)\varphi(t,t_0)} \tag{9}$$

where $\Delta\varepsilon(t)$ and $\Delta\sigma(t)$ = incremental strain and stress of concrete at time t, $\Delta\varepsilon(t) = \varepsilon(t) - \varepsilon(t_0)$, $\Delta\sigma(t) = \sigma(t) - \sigma(t_0)$; $\varepsilon(t)$ and $\sigma(t)$ = total strain and stress of concrete at time t; $E_\varphi(t, t_0)$ = effective elastic modulus of concrete; $\chi(t, t_0)$ = ageing coefficient.

For long-span CFST arch bridges, geometric nonlinearity undoubtedly aggravates the structural creep effects. This paper considers the coupling effect and treats the geometric nonlinearity as a large rotation problem, assuming that the rotations are large but the mechanical strains, those that cause stresses, can be still evaluated by linearized expressions. For the sake of decoupling the kinematical coherency from the elastic response, the corotational approach (Rankin and Brogan 1986, Nour-Omid and Rankin 1991, Felippa and Haugen 2005), developed based on the polar decomposition theorem (Malvern 1969), is adopted. It decomposes displacement field in a deforming body into a rigid body rotation and a strain-producing deformation as

$$[u^{\text{tot}}] = [u^{\text{def}}] + [u^{\text{rig}}] \tag{10}$$

where only $[u^{\text{tot}}]$ causes straining. The principle of this approach is to remove the rigid body contribution $[u^{\text{rig}}]$ before any computations on the element level is undertaken, so as that the remaining deformational displacement $[u^{\text{def}}]$ would be small quantities which fall well within the range for which most elements are designed. To achieve these ends, a local corotational frame that continuously rotates with the element and with respect to which standard, small-strain, small-displacement relationship can be applied is associated with each element. Then the following special form taken on for the strain-displacement relationship contains the information of nonlinearities.

$$[B_n] = [B_v][T_n] \tag{11}$$

where $[B_n]$ = strain-displacement relationship containing the geometric nonlinear information; $[B_v]$ = usual small strain-displacement relationship in the original (virgin) element coordinate system; $[T_n]$ = orthogonal transformation relating the original element coordinates to the rotated element coordinates, which is computed by separating the rigid body rotation from the total deformation.

The governing equation for elements in the finite element model for structural creep analysis is then deduced according to the principle of virtual work and the incremental form of stress-strain relationship involving concrete creep as

$$[K_\varphi^e]\{\Delta\delta^e\} - [K_\varphi^e]\{\delta_{0t}^e\} = \{\Delta F^e\} \tag{12}$$

$$[K_\varphi^e] = \int_e [T_n]^T [B_v]^T [D_\varphi][B_v][T_n]\mathrm{d}V \tag{13}$$

$$\{\delta_{0t}^e\} = \{\delta^e(t_0)\}\varphi(t,t_0) \tag{14}$$

Where $[K_\varphi^e]$ and $[D_\varphi]$ = element stiffness matrix and elasticity matrix reckoning in creep effect respectively, which are achieved by substituting $E_\varphi(t, t_0)$ for the conventional 28-day elastic modulus of concrete; $\{\delta_{0t}^e\}$ = nodal creep displacement at time t due to the initial elastic

displacement; $\{\delta^e(t_0)\}$ = nodal displacement vector at time t_0; $\{\Delta\delta^e\}$ and $\{\Delta F^e\}$ = nodal displacement increment and nodal force increment of element due to creep from t_0 to t, respectively; and the superscript e denotes the vector is expressed in element coordinate system. Consider the item $[K_\varphi^e]\{\Delta\delta^e\}$ in Eq. (12) as an equivalent nodal force of one element due to concrete creep and move it to the right-hand-side of the equation. Note that for global analysis, the sum of the nodal force increment (after being transformed into the global coordinates) of all the elements jointed at one node (except for constraint nodes) is zero, i.e., $\Sigma\{\Delta F\} = 0$, so the unknown $\{\Delta\delta\}$ can be solved as it is just attributed to the transformed equivalent force $\Sigma[K_\varphi^e]\{\Delta\delta_{0t}\}$. Detailed computational method is given in the previous work by Wang *et al*. (2013).

4.3 Equation of motion after creep

As would usually be the case in practice, earthquake occurs long after the completion of a bridge. Without loss of generality, assume that the creep behavior of a structure begins at time t_0, and an earthquake excitation acts on the structure at time t. The dynamic analysis taking into account the influence of concrete creep is in essence to establish and solve the equation of motion of the structure at time t, on the basis of the consideration of the variations in structural configuration and in mechanical properties of concrete material accumulated during t_0 to t (mainly reflected through the treatments on the structural stiffness matrix).

In the case of considering creep effect, the equation of motion of a multi-degree-of-freedom system at time t is

$$[M]\{\ddot{u}\}+[C]\{\dot{u}\}+\left[K^c\right]\{u\}=[P] \tag{15}$$

where $[M]$ and $[C]$ are the mass and damping matrices respectively; $\{u\}$ is the displacement vector; $[P]$ represents the external excitation vector; and $[K^c]$ is the stiffness matrix of the structure at time t with the consideration of creep effect.

As stated above, the influence of creep on the dynamic performance of a structure is originated from two aspects. With regard to the variation in structural configuration caused by creep, creep deformation from t_0 to t is firstly calculated by Eqs. (12)-(14), then added to the original node coordinates to form the updated ones and the structural stiffness matrix at time t. With regard to the variation in concrete elastic modulus, $E_{c,sus}(t, t_0)$ evaluated by Eq. (3) is used, instead of the traditional $E_{c,28}$, to assemble the structural stiffness matrix at time t. These treatments ensure that $[K^c]$ contains the information of creep behavior. Then, solve Eq. (15) following the general method for structural seismic equation, and the solution is the seismic response reckoning in creep influence.

5. Numerical simulation

5.1 Bridge description

A long-span half-through CFST arch bridge, Yajisha Bridge spanning the Pearl River in Guangdong Province, China, is analyzed as a numerical example in this paper. The bridge span arrangement is 76 m + 360 m + 76 m, as sketched in Fig. 1. The effective span and rise of the main arch are 344 m and 76.45 m respectively. Each main arch rib consists of six CFST chords connected by web members, whose typical cross section is shown in Fig. 2. Concrete with
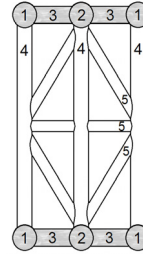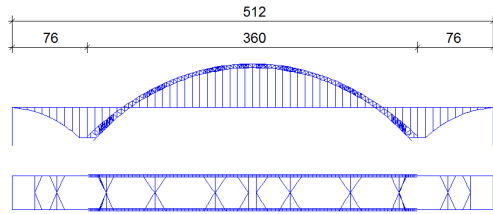
1 side-chord Q345-φ750×18;
2 mid-chord Q345-φ750×20;
3 horizontal web Q345;
4 vertical web Q235-φ450×12;
5 oblique web Q345-φ323.9×10.3

Fig. 1 Elevation and plan view of Yajisha Bridge (unit:m)   Fig. 2 Cross section of main arch rib (unit:mm)

compressive strength of 50 MPa is used in the chords and the horizontal webs, whereas there is no concrete within the vertical and oblique web members and the steel tubes of transverse braces.
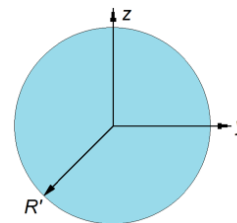
5.2 Finite element modelling

The structural analysis is performed with the finite element analysis code ANSYS. A three dimensional finite element model of the CFST arch bridge was constructed, with the assumption that the steel tube is perfectly bonded to the concrete. The steel tubes and concrete cores of main arch ribs, side arch ribs, web members, transverse braces, spandrel columns, beams and stringers under the bridge deck, tie beams, piers, pile caps and pile foundations were all modeled with two-node beam elements; while the hangers and horizontal cables were modeled with spar elements. The CFST members are simulated by a separated model as depicted in Fig. 3. The initial elastic modulus and mass density of the concrete in the main arch are $3.45×104$ MPa and 2500 kg/m^3; and the elastic modulus and mass density of the steel tube are $2.1×105$ MPa and 7850 kg/m^3 respectively.

The dead loads leading to the creep behavior of the bridge were applied step by step as construction procedure, divided roughly into four stages in this paper, was taken into account by the technique of element birth and death provided in ANSYS. Stage 1 is used for simulating the concrete pouring to the steel tube arch rib, in this stage the concrete is unable to bear any load condition. In the finite element model of stage 1, the element stiffness reduction was multiplied by a near zero coefficient to keep main arch rib concrete element in failure state, so the gravity load was almost entirely borne by the steel tube. In stage 2, activating concrete elements in the main arch rib chord and league, which would lead to stress redistribution between steel tube and concrete members. In stage 3, activating the arch rib, wind support and pier members. Finally, in
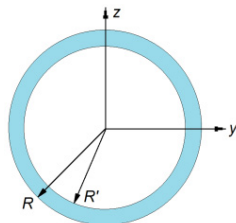
(a) Steel tube   (b) Concrete core
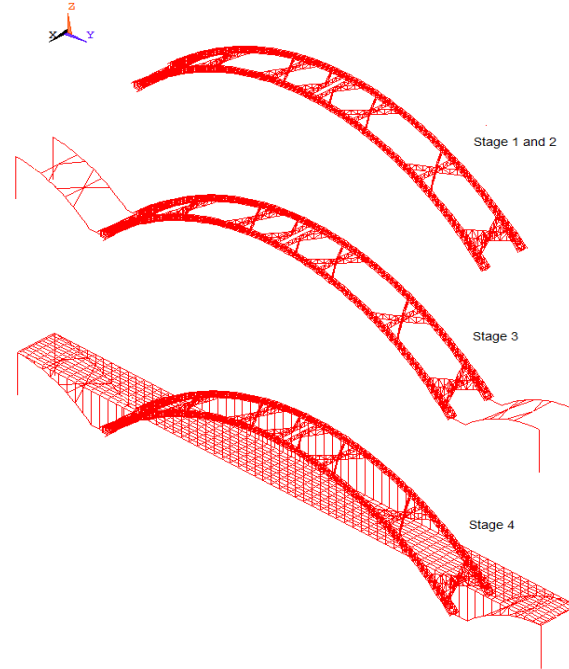
Fig. 3 Separated model of CFST members

Fig. 4 Finite element model of Yajisha Bridge

stage 4, activating boom, columns, tie rod, and the beam members in bridge deck system, which would lead to the redistribution of the initial stress in steel tube and concrete once again. This is quite fundamental because the peculiarity of CFST structures, namely the steel tube acts as not only longitudinal reinforcements but also the concrete formwork needed during construction, results in a comparatively high initial stress in the steel tubes, which affects the stress redistribution during the long-term creep analysis considerably. The finite element models of Yajisha Bridge in different construction stages are illustrated in Fig. 4. Stages 1 to 4 were used to simulate the creep process and Stage 4 was also used to simulate the seismic response.

The El Centro wave was adopted as earthquake excitation. The peak ground acceleration was adjusted to 81.63 cm/s^2, which corresponds to the ground motion with an occurrence probability of 10% during 50 years (Hu *et al*. 2001). The time step was set to be 0.02 s. Assume that the longitudinal, traverse and vertical axes of the bridge coincide with the ground motion axis. In the case of multi-dimensional excitations, the peak acceleration of vertical motion was set to be 2/3 of the horizontal one. The commonly used Rayleigh damping was applied to the model and the damping ratio was valued as 0.02.

5.3 Validation of the computational model

The calculated creep effects at the ages of 180 d and 540 d (from the day that the concrete in the arch ribs began to bear loads) are listed in Table 2, where σ_s and σ_c stand for the stresses in the steel tube and the concrete core at the top point of the arch crown section; Δ_{creep} is the mid-span creep deflection; and $E_{c,sus}$ is the elastic modulus of the concrete after creep. Also tabulated are the in-site measurements (Xin and Xu 2003), which are in good agreement with the calculated values.

Table 2 Comparison between prediction and measurement of creep effects of Yajisha Bridge

	180 d			540 d		
	Measurement	Prediction	Error	Measurement	Prediction	Error
σ_s (MPa)	206.4	212.4	2.91%	218.3	218.4	0.05%
σ_c (MPa)	13.8	11.7	15.2%	11.3	11.1	1.77%
Δ_{creep} (m)	----	0.091	----	0.120	0.114	5.00%
$E_{c,sus}$ (MPa)	----	3.88×10^4	----	----	3.99×10^4	----

5.4 Influence of creep on natural frequencies

The development of the natural frequencies of Yajisha Bridge with the time of creep is presented in Fig. 5. All these curves were calculated with $E_{c,sus}(t, t_0)$ and the structural configuration after creep. The natural frequencies of the CFST arch bridge go up gradually with the increase of the load-keeping time. After 3000 days of creep, the frequencies of the 1st, 3rd and 5th modes of vibration rise by 2.85%, 5.79% and 4.46% respectively. It has been demonstrated that the vibration modes of long-span CFST arch bridges distribute quite densely within a narrow frequency range. In this context, the error induced by ignoring the creep influence might exceed the difference between two adjacent frequencies, which highlights the significance of taking the creep effect into account.

5.5 Influence of creep on dynamic responses

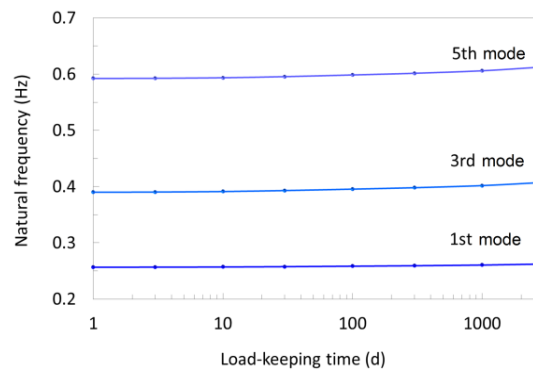The influence of creep on the seismic response of the CFST arch bridge is investigated based


Fig. 5 Evolution curves of natural frequencies

Table 3 Loading cases of the seismic analysis of Yajisha Bridge

Loading case	Wave speed (m/s)	Excitation orientation	Ratio of peak acceleration
1	∞	longitudinal	--
2	∞	longitudinal + vertical	1:2/3
3	∞	longitudinal + traverse + vertical	1:1:2/3
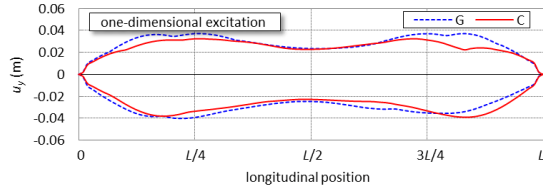
Fig. 6 Enveloping diagram of u_y under loading case 1
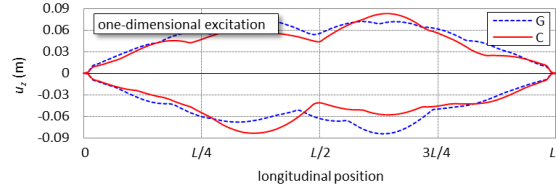
Fig. 7 Enveloping diagram of u_z under loading case 1
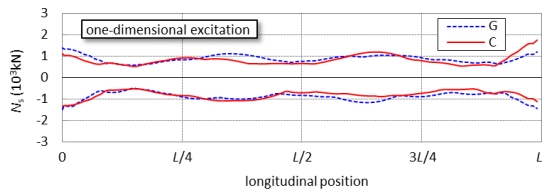
Fig. 8 Enveloping diagram of N_s under loading case 1
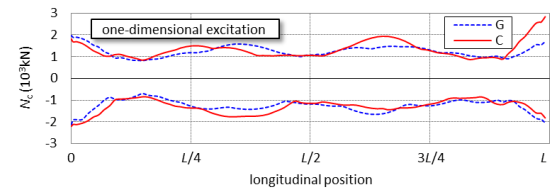
Fig. 9 Enveloping diagram of N_c under loading case 1
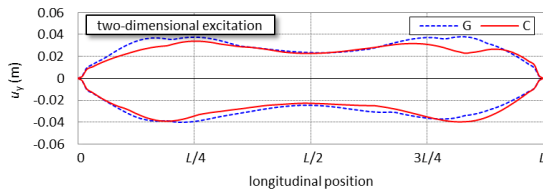
Fig. 10 Enveloping diagram of u_y under loading case 2
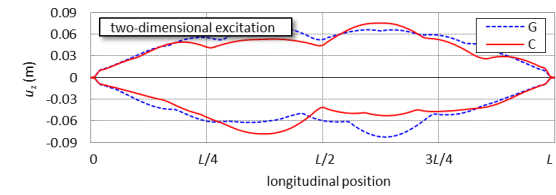
Fig. 11 Enveloping diagram of u_z under loading case 2
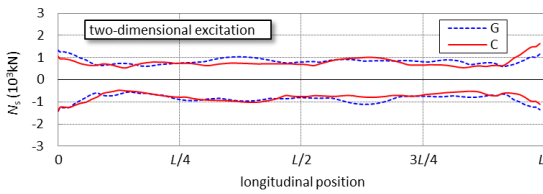
Fig. 12 Enveloping diagram of N_s under loading case 2
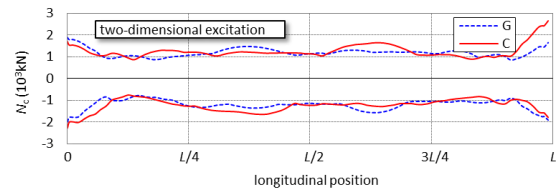
Fig. 13 Enveloping diagram of N_c under loading case 2
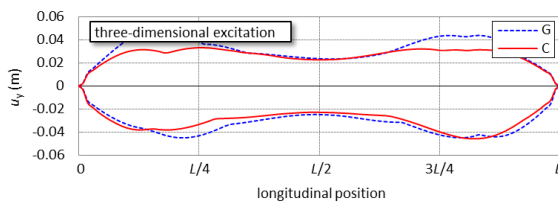
Fig. 14 Enveloping diagram of u_y under loading case 3
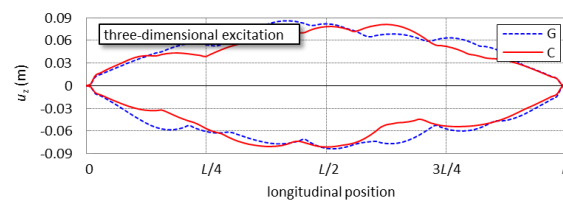
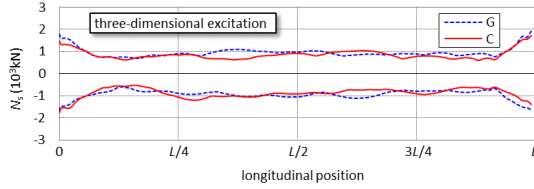Fig. 15 Enveloping diagram of u_z under loading case 3

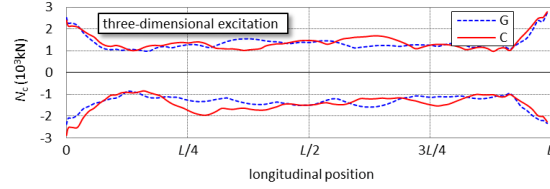Fig. 16 Enveloping diagram of N_s under loading case 3

Fig. 17 Enveloping diagram of N_c under loading case 3

on the results of time-history analyses under three different excitations, which are specified in Table 3. Comparisons of the displacement and axial force enveloping curves between the two cases of considering creep effect or not are shown in Figs. 6-17, where curve C stands for the results of the seismic analyses considering one year's creep effect, while curve G stands for those only considering gravity effect. Illustrated responses include the longitudinal displacement u_y, the vertical displacement u_z, the axial forces of the steel tube N_s and of the concrete N_c. Note that the responses shown in the following figures are of the upper rib, and geometric nonlinearity is taken into account in all calculations.

From the displacement enveloping diagrams, changes in the response amplitude take place due to creep under all the three loading cases, so as to make that the maximum and minimum values in certain ranges (0~L/4 and 3L/4~L for the longitudinal displacement; L/4~L/2 and L/2~3L/4 for the vertical displacement) exceed the enveloping limits which only consider gravity effect. Under the one-dimensional excitation, the amplitudes of the longitudinal and vertical displacements with creep effect respectively exceed by 32.54% (around 7L/8) and 33.04% (around 3L/8) at most; under the two-dimensional excitation, they respectively go beyond by 20.06% (around 7L/8) and 32.98% (around 3L/8) at most; while under the three-dimensional excitation, the biggest discrepancies in the amplitudes of the longitudinal and vertical displacements between the two cases are 12.46% (around L/8) and 20.77% (around 5L/8).

From the axial force enveloping diagrams, we can see that the amplitudes of the axial forces near the arch springing, which is the control section under a seismic effect for CFST arch bridges, increase considerably due to creep. Compared to the enveloping values considering only gravity effect, under the one-dimensional excitation, creep effect makes the maximum tensile forces of the steel tube and the concrete at the right arch springing increase by 46.09% and 67.14% respectively; under the two-dimensional excitation, the corresponding responses of the steel tube and the concrete rise due to creep by 40.54% and 60.79% respectively; while under the three-dimensional excitation, the maximum compressive force of the concrete at the left arch springing increases by 21.26%.

Creep effect also causes the amplitudes of the axial forces at the middle part of the arch rib to change obviously. Under the one-dimensional excitation, the maximum tensile force of the steel tube goes up by 19.58% due to creep around 5L/8, and the maximum tensile and compressive forces of the concrete increase by 36.80% around 5L/8 and 33.17% around 3L/8 respectively; under the two-dimensional excitation, the corresponding response of the steel tube goes up by 19.53% around 5L/8 due to creep, and the corresponding responses of the concrete increase by 45.34% around 3L/16 and 28.39% around 3L/8 respectively; while under the three-dimensional excitation, the steel tube has an increase of 29.36% in the maximum compressive force around L/4 due to creep, and the concrete has increases of 43.36% (around 5L/8) and 48.00% (around L/4) in the maximum tensile and compressive forces.

6. Conclusions

This paper analyzes the relationships between sustained load and instantaneous load, static behavior and dynamic behavior, and long-term effect and instantaneous response, and explains the influencing mechanism of creep on structural dynamic behavior. The concept of after-effect of creep is proposed in this paper to describe the phenomenon that the mechanical properties of concrete change after a period of creep. The predictive formula of the elastic modulus of concrete after creep is given based on available test data.

The sustained loading in prior to an earthquake results in changes in the configuration and stiffness of CFST arch bridges, and further influences the dynamic property and seismic responses of the bridges. The natural frequencies of CFST arch bridges increase when creep effect is taken into account, and they go up gradually with the increase of load-keeping time. The change in the seismic responses of the displacement and internal force due to creep is not negligible; otherwise the responses of some sections will be underestimated. The creep influence is related closely to the excitation and the structure, and should be analyzed case-by-case.

Acknowledgments

References

Aldemir, U., Yanik, A. and Bakioglu, M. (2012), "Control of structural response under earthquake excitation", *Comput.-Aided Civil Infra. Eng.*, **27**(8), 620-638.

Alizadeh, R., Beaudoin, J.J. and Raki, L. (2010), "Viscoelastic nature of calcium silicate hydrate", *Cement Concrete Compos.*, **32**(5), 369-376.

Bažant, Z.P. (1972), "Prediction of concrete creep effects using age-adjusted effective modulus method", *J. Am. Concrete Inst.*, **69**(20), 212-217.

Bažant, Z.P. (1988), *Mathematical Modeling of Creep and Shrinkage of Concrete*, John Wiley & Sons, Chichester and New York, NY, USA.

Bažant, Z.P. and Baweja, S. (2000), "Creep and shrinkage prediction model for analysis and design of concrete structures: Model B3", *ACI Special Publications*, **194**, 1-84.

Bažant, Z.P. and Prasannan, S. (1989a), "Solidification theory for concrete creep. I: Formulation", *J. Eng. Mech.*, **115**(8), 1691-1703.

Bažant, Z.P. and Prasannan, S. (1989b), "Solidification theory for concrete creep. II: Verification and application", *J. Eng. Mech.*, **115**(8), 1704-1725.

Cook, D.J. and Chindaprasirt, P. (1980), "Influence of loading history upon the compressive properties of concrete", *Mag. Concrete Res.*, **32**(111), 89-100.

Davis, R.E. and Davis, H.E. (1931), "Flow of concrete under the action of sustained load", *J. Am. Concrete Inst.*, **2**(7), 837-901.

Fédération Internationale du Béton (FIB) (2010), CEB-FIP Model Code 2010.

Felippa, C.A. and Haugen, B. (2005), "A unified formulation of small-strain corotational finite elements: I. Theory", *Comput. Method. Appl. Mech. Eng.*, **194**(21-24), 2285-2335.

Ghodrati Amiri, G., Abdolahi Rad, A. and Khorasani, M. (2012), "Generation of Near-Field Artificial Ground Motions Compatible with Median Predicted Spectra Using PSO-based Neural Network and Wavelet Analysis", *Comput.-Aided Civil and Infrastructure Engineering*, **27**(9), 711-730.

Graf, W., Freitag, S., Kaliske, M. and Sickert, J.U. (2010), "Recurrent neural networks for uncertain time-dependent structural behavior", *Computer-Aided Civil Infra. Eng.*, **25**(5), 322-333.

Hu, S.D., Wang, J.J., Wei, H.Y. and Ye, A.J. (2001), "Seismic behavior analysis of Yajisha Bridge", *Railway Standard Design*, **21**(6), 21-25.

Huang, R.Y., Mao, I.S. and Lee, H.K. (2010), "Exploring the Deterioration Factors of Bridges: A Rough Set Theory Approach", *Computer-Aided Civil Infra. Eng.*, **25**(7), 517-529.

Ma, Y.S. (2013), "Creep influence on static and dynamic reliability of long-span concrete filled steel tube arch bridges", Ph.D. Dissertation; Beijing Jiaotong University, Beijing, China.

Ma, Y.S. and Wang, Y.F. (2013), "Creep effects on the reliability of concrete-filled steel tube arch bridge", *J. Bridge Eng.*, **18**(10), 1-10.

Ma, Y.S., Wang, Y.F. and Mao, Z.K. (2011), "Creep effects on dynamic behavior of concrete filled steel tube arch bridge", *Struct. Eng. Mech., Int. J.*, **37**(3), 321-330.

Malvern, L. (1969), *Introduction to the Mechanics of a Continuous Medium*, Prentice Hall, New York.

Naguib, W. and Mirmiran, A. (2003), "Creep modeling for concrete-filled steel tubes", *J. Construct. Steel Res.*, **59**(11), 1327-1344.

Nour-Omid, B. and Rankin, C.C. (1991), "Finite rotation analysis and consistent linearization using projectors", *Comput. Method. Appl. Mech. Eng.*, **93**(3), 353-384.

O'Byrne, M., Schoefs, F., Ghosh, B. and Pakrashi, V. (2013), "Texture Analysis Based Damage Detection of Ageing Infrastructural Elements", *Computer-Aided Civil Infra. Eng.*, **28**(3), 162-177.

Qin, J. and Faber, M.H. (2012), "Risk management of large RC structures within a spatial information system", *Computer-Aided Civil Infra. Eng.*, **27**(6), 385-405.

Rankin, C.C. and Brogan, F.A. (1986), "An element independent corotational procedure for the treatment of large rotations", *J. Press. Vessel Technol.*, **108**(2), 165-174.

Sapountzakis, E.J. and Katsikadelis, J.T. (2003), "Creep and shrinkage effect on the dynamic analysis of reinforced concrete slab-and-beam structures", *J. Sound Vib.*, **260**(3), 403-416.

Shao, X.D., Peng, J.X., Li, L.F., Yan, B.F. and Hu, J.H. (2010), "Time-dependent behavior of concrete-filled steel tubular arch bridge", *J. Bridge Eng.*, **15**(1), 98-107.

Terrey, P.J., Bradford, M.A. and Gilbert, R.I. (1994), "Creep and shrinkage of concrete in concrete-filled circular steel tubes", *Proceeding of 6th International Symposium on Tubular Structures*, Melbourne, Australia, December.

Wang, Y.F. and Zhang, D.J. (2009), "Creep-effect on mechanical behavior of concrete confined by FRP under axial compression", *J. Eng. Mech.*, **135**(11), 1315-1322.

Wang, Y.F., Han, B. and Zhang, D.J. (2008), "Advances in creep of concrete filled steel tube members and structures", *Proceeding of 8th Concreep Conference*, Ise-Shima, Japan, October, pp. 595-600.

Wang, Y.F., Ma, Y.S., Han, B. and Deng, S.Y. (2013), "Temperature effect on creep behavior of CFST arch bridges", *J. Bridge Eng.*, **18**(12), 1397-1405.

Washa, G.W. and Fluck, P.G. (1950), "Effect of sustained loading on compressive strength and modulus of elasticity of concrete", *J. Am. Concrete Inst.*, **21**(9), 693-700.

Wu, Q.X., Yoshimura, M., Takahashi, K., Nakamura, S. and Nakamura, T. (2006), "Nonlinear seismic properties of the Second Saikai Bridge: A concrete filled tubular (CFT) arch bridge", *Eng. Struct.*, **28**(2), 163-182.

Xin, B. and Xu, S.Q. (2003), "Creep analysis of long-span concrete filled steel tube arch bridges", *Railway Standard Design*, **4**, 31-33.

Zhang, D.J., Wang, Y.F. and Ma, Y.S. (2010), "Compressive behaviour of FRP-confined square concrete columns after creep", *Eng. Struct.*, **32**(8), 1957-1963.

CC